Transport and Communications Science Journal

# A HIGH GAIN WIDEBAND ARRAY ANTENNA BASED ON METASURFACE FOR ETC APPLICATION

**Khuat Dinh Chinh, Tran Thi Lan***

University of Transport and Communications, No 3 Cau Giay Street, Hanoi, Vietnam

ARTICLE INFO

TYPE: Research Article
Received: 18/05/2022
Revised: 29/07/2022
Accepted: 10/08/2022
Published online: 15/09/2022
https://doi.org/10.47869/tcsj.73.7.5

* *Corresponding author*
Email: ttlan@utc.edu.vn; Tel: +84 975080388

**Abstract.** Free flow electronic toll collection (FFETC) has played an important role in building convenient and safe transportation systems in many countries. The most challenging problem when researching and developing this system is shortening the payment cycle so that vehicles passing through the stations do not need to stop or keep going at a speed greater than 60 Km/h. Designing roadside unit (RSU) reader antennas with high gain and suitable radiation pattern is the most feasible and economical solution. This paper proposes a left-handed circularly polarized (LHCP) 2×4 array antenna using sequential phase rotation power dividers at 5.8 GHz band. The element antenna is a square patch antenna with a slit in the middle for better impedance matching, six trapezoidal parasitic patches added to either side of the main patch to create resonance at high frequencies, and a metasurface placed on top of the main patch. The proposed metasurface is a 4×4 array of dual circular unit cells to improve gain and extend axial ratio (AR) bandwidth. The proposed antenna array has a high gain of 17 dBi, -3 dB vertical and horizontal beamwidths of $33.2^0$ and $17.1^0$, which cover over one lane, are expected for any ETC system to avoid interference with other lanes. Impedance bandwidth and AR bandwidth are 2.19 GHz (37.75%) and 2.06 GHz (35.52%), respectively. The overall dimensions of the proposed array antenna are approximately 152×76×6.4 $mm^3$. With the above merits, this antenna is a suitable candidate for the RSU reader antenna in the FFETC.

**Keywords:** Array antenna, circular polarization, FFETC, metasurface, sequential feeding network, parasitic patch.

## 1. INTRODUCTION

Traffic currently has a number of problems such as accidents, environmental pollution, congestion affecting all aspects of society. From those problems, the intelligent transportation system (ITS) has been gradually developed to build a safe, sustainable, convenient and environmentally friendly transportation system. One of the applications of ITS is free-flow electronic toll collection (FFETC) using the dedicated short-range communication standard (DSRC). The structure of the FFETC system consists of OBU (On-Board Unit) mounted on the window of vehicles and RSU (Road Side Unit) installed at a toll station on the highway. The RSU's task is to communicate with the OBU to receive vehicle information through the dedicated short-range communication (DSRC) standard. DSRC is a technology with high transmission speed, security and accuracy compared to previous technologies (e.g. RFID) [1]. Therefore, this technology is used in many countries around the world.

In the US, the Federal Communications Commission (FCC) has allocated 75 MHz in the 5.9 GHz band in ITS applications while the European Telecommunications Standards Institute (ETSI) has established DSRC standards including EN12253 [2] and EN302571 [3]. For RSUs, the EN12253 standard stipulates that the antenna must have a bandwidth of 20 MHz around 5.8 GHz. The vertical and horizontal beamwidths should be $15^0$ and $30^0$, respectively [10]. The standard also requires that the sidelobe level is at least 15 dB lower than those of the bore sight. The polarization of the antenna is left circular polarization (LHCP) with polarization isolation of at least 15 dB. Next, EN302571 - ITS DSRC operates at 5.9 GHz, using a bandwidth of 70 MHz.

The biggest challenge in studying the FFETC system was implementing a fast payment cycle of no more than 200 ms [4]. To meet this speed, we can optimize the data transmission process of the RSU or increase the clock frequency. However, this solution increases the price of the RSU, and the peak clock frequency does not exceed 100MHz. Another potential solution is to design an antenna for the RSU with high gain and suitable transmission range to cover the vehicle's mileage in one billing cycle. The antenna transmission range which depends on gain, vertical and horizontal beamwidths need to be determined based on the payment cycle time and vehicle speed through the RSU.

Recently, there have been a number of studies that have proposed DSRC antennas in ETC systems. In [4], a 2×2 array antenna is proposed using a sequential phase rotation power divider with a dual fed element antenna to create circular polarization. The antenna has a gain of 13dBi, which is quite low compared to the current RSU antenna requirements. Moreover, narrow bandwidth is another disadvantage of this antenna. To achieve a higher gain, an array antenna was proposed in [5]. Although the gain is higher, the antenna size is large and bandwidth is narrow about 1%. On the other hand, a low-profile helix antenna mentioned in [6] uses an artificial magnetic conductor (AMC) placed below the antenna. In addition, above the antenna, a frequency selective surface (FSS) is used to increase the radiated aperture of the antenna, so that the gain of the antenna is improved but the bandwidth 2.58% is quite narrow and it is linearly polarized. At the same time, the disadvantage is large height because of the use of helix antenna. In [7], a five-element array is proposed. There are four patches placed in the four corners and one patch is placed in the center of the array and it is powered with twice the capacity of the surrounding patches. Its impedance bandwidth and AR bandwidth respectively are 4.48% and 2.58% wider than above-mentioned antennas but the slidelobe level of -12.5 dB is high. The antenna in [8] has some advantages such as wide AR

bandwidth of 19.4 %, high gains at 5.8GHz and 5.9GHz are respectively 14.7 dBi and 17 dBi, but the symmetric radiation pattern has main beamwidths around $22^0$ which is not expected for ETC antennas. In [9], a high gain Fabry-Perot resonant antenna is proposed, consists of two layers. The lower layer is a microstrip antenna and the upper layer is an FSS consisting of an 8×8 array of metal unit cells to increase gain and bandwidth. The simulation results show that the antenna has an high gain of 18 dBi but the bandwidth of 4.3% is narrow. Also, its radiation pattern has not been optimized to cover a single lane. A DSRC transponder in [10] had optimized radiation patterns with $30^o$ and $15^0$ in horizontal and vertical planes suitable for the Europe standard. However, bandwidth is narrow, not suitable for future applications. Therefore, this study try to design an RSU array antenna meeting the European DSRC standard with high gain, wideband, and beamwidths big enough to cover a single lane. To obtain these goals, the proposed array antenna consists of element antennas which are microstrip antennas cut at two corners with parasitic patches. To enhance gain and AR bandwidth, a nut-shaped metasuface is designed to place above the antenna. The size of the proposed array antenna is reduced by using sequential-phase feeding network.

The content of the paper will be organized as follows: The structure and design principle of the element antenna is presented in Section 2. In Section 3, the proposed array antenna with the sequential-phase feeding network is described. Finally, some conclusions and future works are given in Section 4.

## 2. ELEMENT ANTENNA DESIGN

### 2.1. Structure of the proposed element antenna

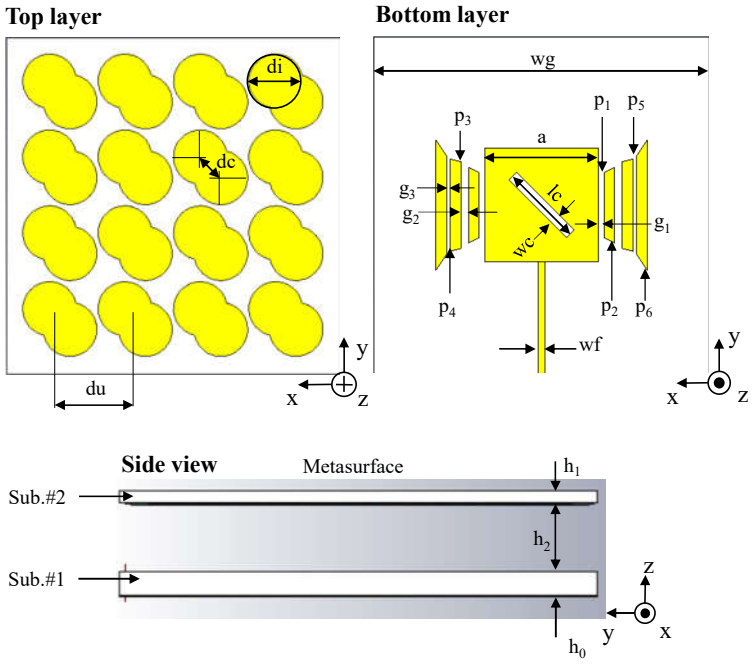


Figure 1. Structure of the proposed element antenna ($h_0$ = 1.53, $h_1$ = 0.73, $h_2$ = 4, $du$ = 7, $dc$ = 2, $di$ = 5, $w_g$ = 31, $p_1$ = 6, $p_2$ = 7, $p_3$ = 8, $p_4$ = 8.5, $p_5$ = 9, $p_6$ = 12, $wc$ = 1, $lc$ = 7.5, $g_1$ = 0.5, $g_2$ = 0.7, $g_3$ = 0.3, $w_f$ = 0.7, $a$ = 10.5 (Unit: mm)).

The complete structure of the element antenna depicted in Figure 1 consists of two layers. The lower layer is a linearly polarized microstrip antenna whose substrate layer is FR4 with dielectric constant $\varepsilon_r = 4.3$, tangential loss $\delta = 0.0019$. The element antenna is a square patch with a diagonal slit. Six trapezoidal parasitoid plates were placed on either side of the main radiation patch to increase the bandwidth of the element antenna. The upper layer is a polarization reconfigured metasurface, which consists of sixteen-unit cells arranged in a 4×4 layout. Each unit cell has a stacked double circle shape like nut shape.

### 2.2. Analysis of the element antenna

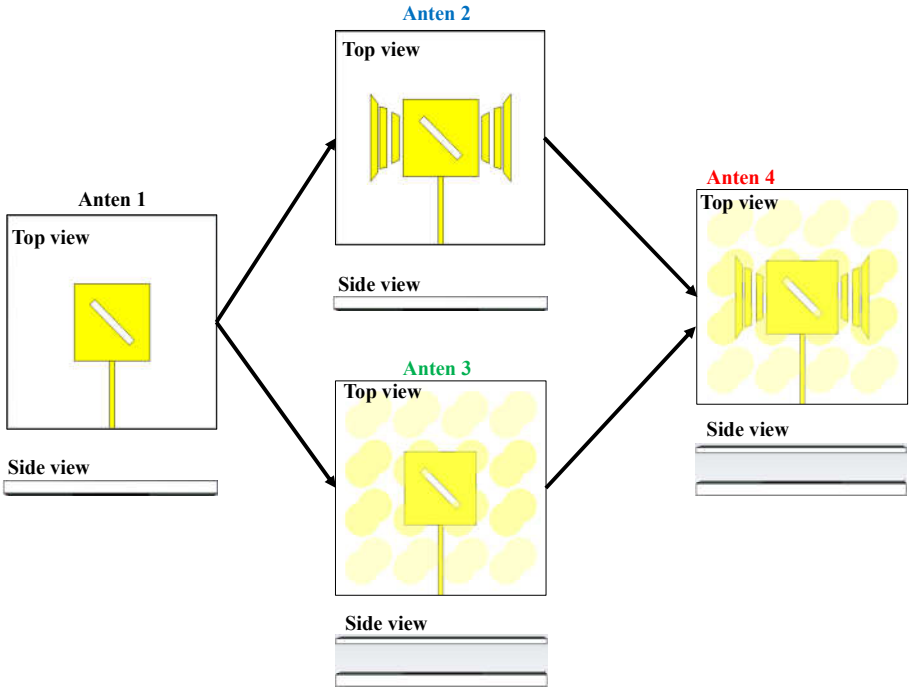


Figure 2. Four versions of the element antenna structure.

This part analyses design process of the element antenna through four versions as shown in Figure 2, and simulation results of these versions are shown in Figure 3. Antenna 1 is the simplest model consisting of a square patch cut diagonally in the middle. Antenna 2 adds six trapezoidal parasitic plates on Antenna 1 while Antenna 3 has a polarization conversion metasurface on top of Antenna 1. Antenna 4 is a combination of both Antenna 2 and Antenna 3. From the results in Figures 3(a) and 3(b), it can be seen that Antenna 1 resonates at 6 GHz and has linear polarization. Thanks to the parasitic plates, Antenna 2 resonates at higher frequency to widen bandwidth. The AR of Antenna 2 are also reduced with 10.9 dB and 8.14 dB at 5.8 GHz and 7.28 GHz, respectively. Due to the capacitive coupling between the main patch and the parasitic elements, the phase difference between the currents on the main patch reaches to $90^0$. As a result, the axis ratio is reduced. However, these first two antennas have very narrow bandwidths and both radiate elliptical polarized waves. Meanwhile, Antenna 3

has the wider impedance bandwidth of 976.9 MHz (16.84%) and the AR is significantly reduced from 12.8 dB to 4.42 dB at 5.8 GHz. This AR reduction is thanks to the proposed metasurface, which changes amplitude and phase electrical field density vectors of elliptically polarized waves to be equal and phase difference of $90^0$ to obtain circular polarization. But, this antenna has not really radiated circularly polarized waves. Finally, Antenna 4 gives the best results when the impedance bandwidth is extended from 5.06 GHz to 7.1 GHz (35.17%) and the AR bandwidth is 23.79%. Thus, it is found that the combination of the metasurface [11] and the parasitic plates [12] contributes to bandwidth improvement and the circular polarization purity of the element antenna. Moreover, the results in Figures 3(c) and 3(d) show that the efficiency and the gain of the element antenna are improved when the parasitic plates and the metasurface are added. In detail, Antenna 4 has stable gain and efficiency in the operating frequency range. The gain of Antenna 4 is higher than 7.5 dBi, and the efficiency is higher than 80%.

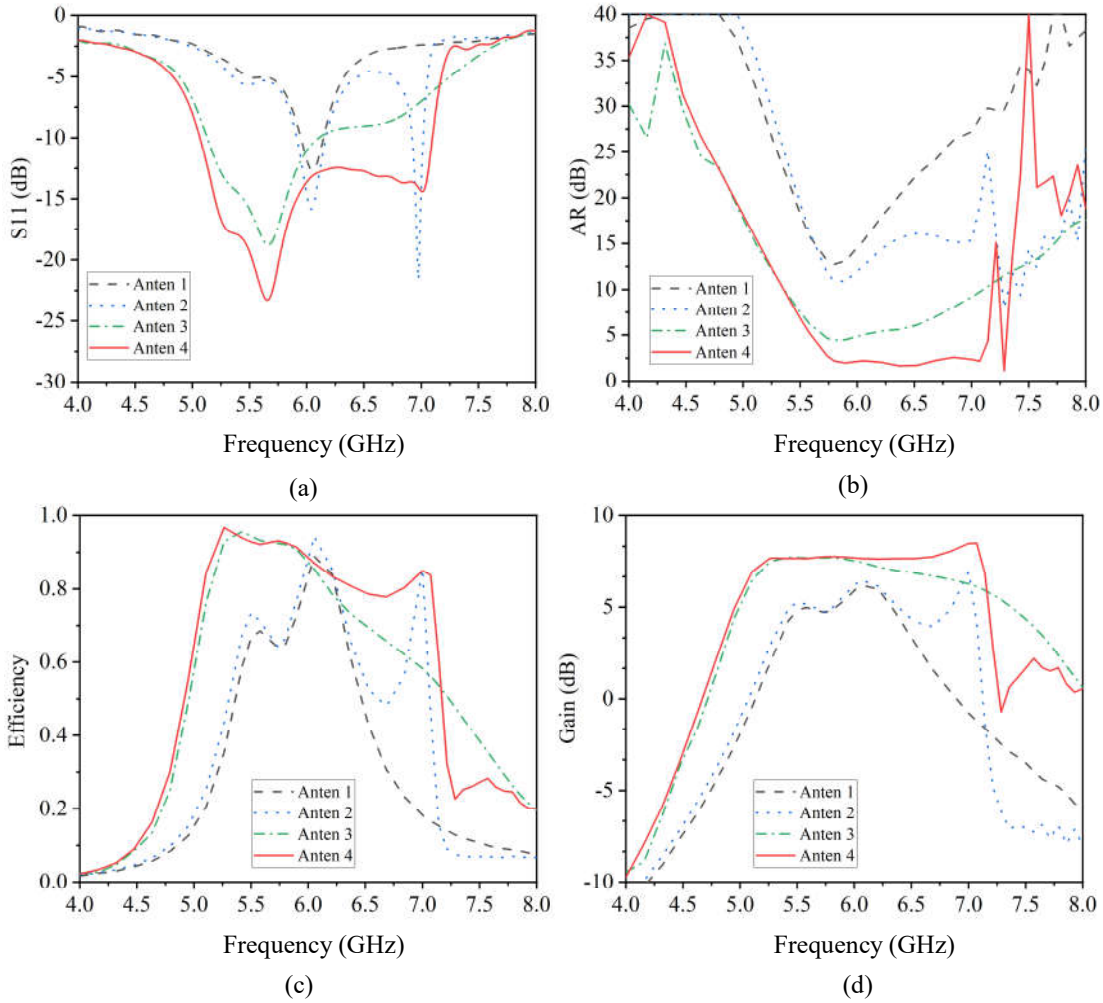


Figure 3. Simulation results of four versions of the element antenna : (a) S11, (b) AR, (c) Efficiency and (d) Gain.

## 3. ARRAY ANTENNA DESIGN

### 3.1. Sequential feeding network

Sequential feeding network are commonly used to fabricate circularly polarized antenna arrays with high gain, high polarization purity and reduction of antenna size [13]. Thus, this sequential feeding network structure is applied in this proposed array antenna. The feeding network shown in Figure 4 consists of four impedance converting segments λ/4, of which three segments are generated based on a circle of radius R = λ/2π with different impedance values. The input of the feeding network is connected to a 50 Ω coaxial cable while the four outputs are connected to 100 Ω lines. The size of the quarter wavelength impedance matching segments is $w_1$, $w_2$, $w_3$, $w_4$, where the length of the first segment is $l_0$.

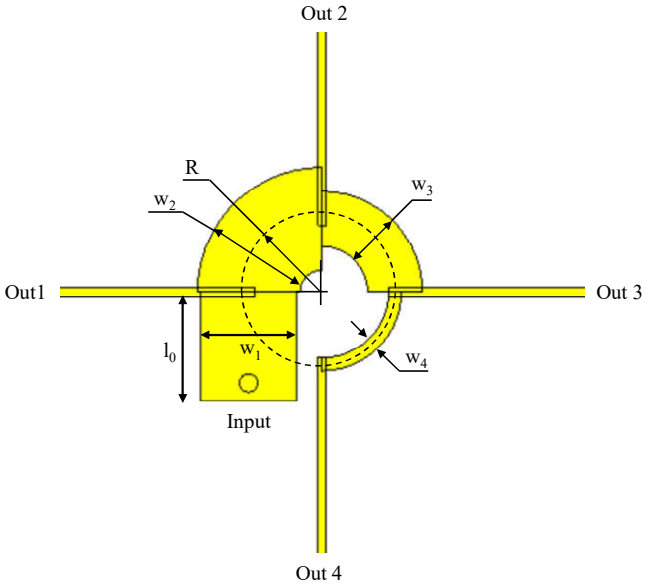


Figure 4. Structure of sequential feeding network ($R$ = 4, $l_0$ = 6, $w_1$ = 5.2, $w_2$ = 5.6, $w_3$ = 3, $w_4$ = 0.3 (Unit: mm).

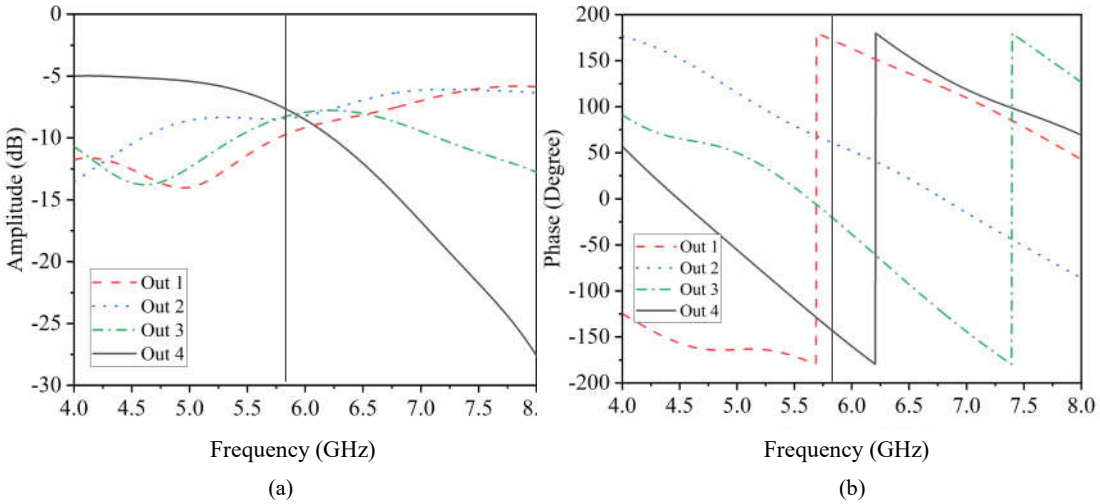


(a) (b)

Figure 5. Simulation results of power divider: (a) Amplitude, (b) Phase.

Figure 5 shows simulation results of the feeding network in terms of amplitude and phase. In Figure 5(a), it can be seen that the power delivered to the Out 1, Out 2, Out 3, Out 4 output ports is -9.84dB, -8.44dB, -8.34dB and -7.5dB, respectively. Figure 5(b) depicts the output signal phase at four ports, from which phase difference between Out 2, Out 3, Out 4 and Out 1 is $112^0$, $192^0$, $311^0$, respectively. Whereas the theoretical output power amplitude at the ports is expected to be equal and the phase difference between Out 2, Out 3, Out 4 and Out 1 is desired to be $90^0$, $180^0$, $270^0$. Therefore, it can be seen that the output power amplitude of ports are well designed. But, the phase difference between Out 2, Out 3, Out 4 and Out 1 needs to be slightly adjusted and this will be considered when the feeding network is combined with element antennas by adding stubs in Section 3.2.

### 3.2. The proposed array antenna

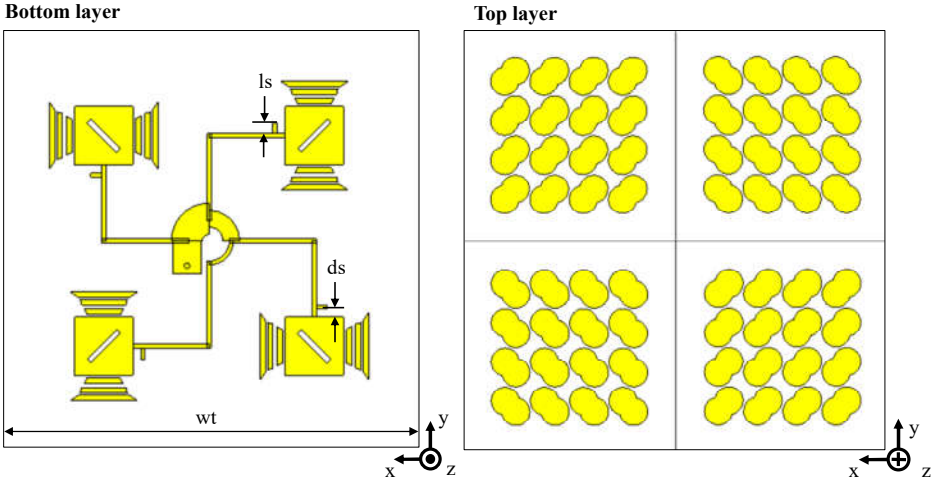


Figure 6. Structure of 2×2 antenna array (*ls* = 2, *ds* = 1.5 and *wt* = 76. Unit: mm).

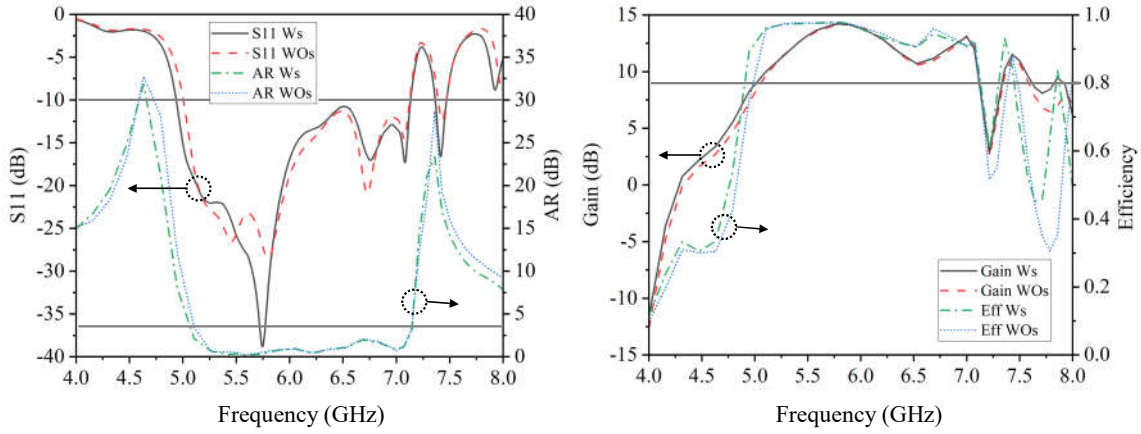


Figure 7. Simulation results of 2×2 antenna array: (a) S11 and AR (b) Broadside gain and efficiency in two cases: with and without stubs (Ws and WOs).

The array antenna is first designed in 2×2 layout using the feeding network in Section 3.1. The array antenna structure is shown in Figure 6. The input of the feeding network is

connected to a 50 Ω coaxial cable, the outputs are connected to four radiating patches by 100 Ω feeding lines. Four stubs are added to the feeding lines for impedance matching and sidelobe reduction in radiation pattern of this antenna. The length of stubs is 2 mm, and stub-to-antenna distance is 1.5 mm. Figure 7(a) show results in two cases with (Ws) and without stubs (WOs). It can be seen that both impedance bandwidth and AR bandwidth are slightly expanded when the stubs are added. Specifically, the impedance bandwidth increases from 36.55% to 37.75% whereas AR bandwidth is improved 1.5 %. The array antenna gain at 5.8 GHz is 14.2 dBi and the efficiency > 80% bandwidth is 2.22 GHz as shown in Figure 7(b). This array antenna has some merits to meet requirements for ETC systems but its radiation pattern (Figures 8, 9) is symmetrical with the beamwidth of $33.3^0$, not satisfied the standard in [10].

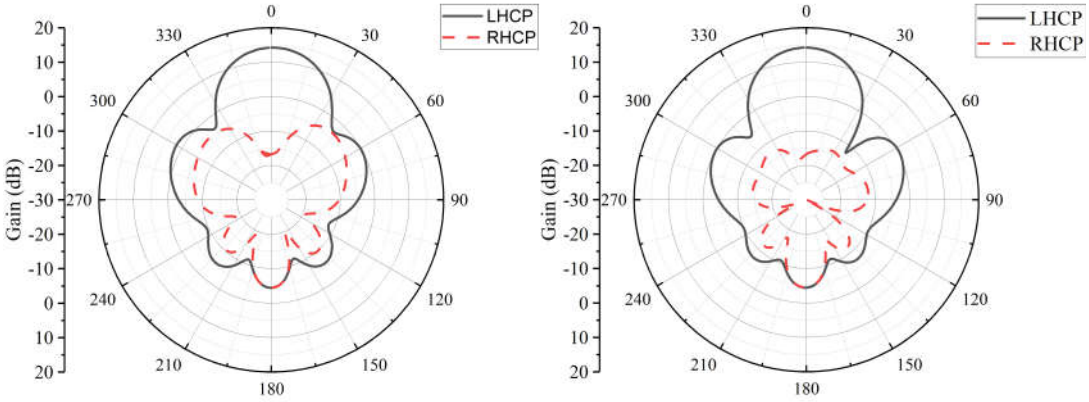


Figure 8: Simulated 2-D radiation pattern of 2×2 array at 5.8 GHz: (a) $\varphi = 0^0$, (b) $\varphi = 90^0$.

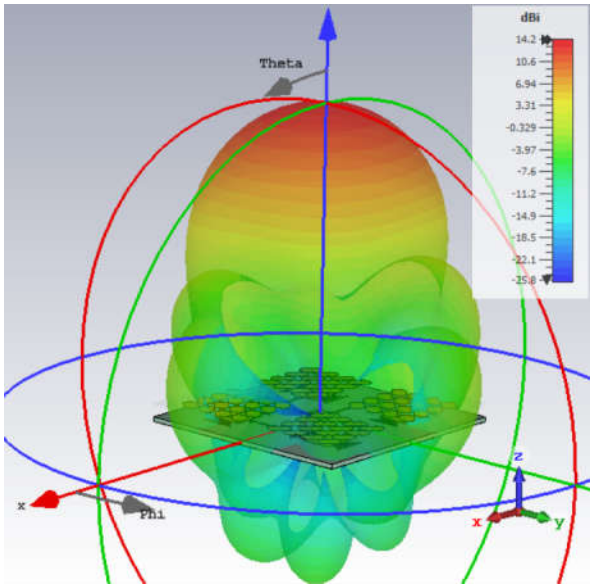


Figure 9: Simulated 3-D radiation pattern of 2×2 array at 5.8 GHz.

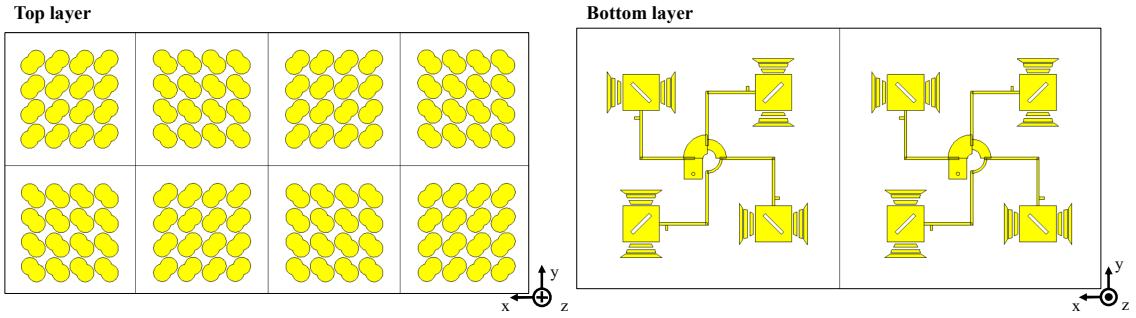


Figure 10. Structure of the 2×4 proposed antenna array.

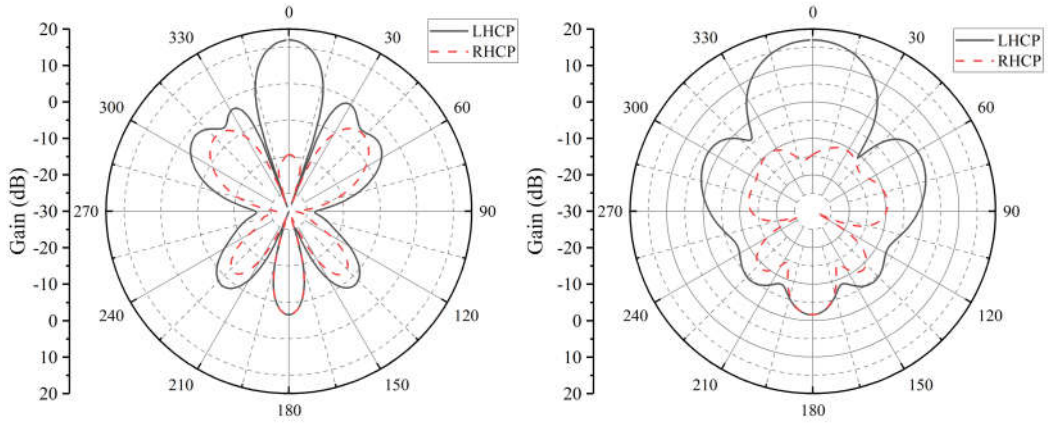


(a) (b)

Figure 11. Simulated 2-D radiation pattern at 5.8 GHz: (a) φ = 0°, (b) φ = 90°.

Table 1. A comparation between the proposed array antenna with other studies.

| References | S11 BW (%) | AR BW (%) | Gain (dBi) | V – H Pattern (degree) | Size (mm) |
|---|---|---|---|---|---|
| **[4]** | 1.37 | Not mentioned | 13 | Not mentioned | Not mentioned |
| **[5]** | 1 | Not mentioned | 14.9 | 32.3-32.7 | 390×340×0.8 |
| **[6]** | 2.58 | Not CP | 12 | 40-40 | 103×103×12.9 |
| **[7]** | 34.48 | 19.4 | 14.7 | 23-23 | 172.8×172.8×0.787 |
| **[8]** | 4.48 | 2.58 | 13.8 | 32-32 | Not mentioned |
| **[9]** | Not mentioned | 19.4 | 18 | 20-20 | Not mentioned |
| **This work** | 37.75 | 35.52 | 17 | 33.2-17.1 | 152×76×6.4 |

Next, the proposed array antenna is designed based on the mentioned-above 2×2 array antenna to satisfy the beamwidths as mentioned in [10]. The radiation patterns in Figures 10, 11 show that the proposed array antenna has gain of 17 dBi and beamwidths at two planes φ = $0^0$ and φ = $90^0$ are $17.1^0$ and $33.2^0$, respectively. The circular polarization isolation at the main beam is 36 dB which represents a high-purity LHCP antenna. Thus, the proposed array antenna is a very good candidate for FFETC application.

## 4. DISCUSSION AND CONCLUSION

To verify the performance of the proposed array antenna, Table 1 is given to compare the proposed antenna with other studies that have been published recently. It can be seen that the antennas reported in [4-8] have a smaller gain than the proposed antenna. The antenna in [9] has a higher gain than the proposed antenna but its size is larger. In terms of bandwidth, antennas in [4-9] are narrower than that of the proposed antenna. Most of the previous antennas have not optimized radiation patterns to be suitable for practical application. Their radiation patterns are all symmetric while the proposed array antenna has radiation pattern satisfied the requirement in [10]. The beamwidths at two planes $\varphi = 0^0$ and $\varphi = 90^0$ are respectively $17.1^0$ and $33.2^0$, which cover enough for one lane. The size of the proposed array antenna in length and width is smaller than those of antennas in [5][7] and is lower than the antenna in [6]. From the above analysis, the proposed array antenna was verified with some advantages such as wide bandwidth, high gain, optimized radiation patterns and compact size. Thus, the proposed array antenna is suitable for FFETC practical system. In future work, the sidelobe level of the proposed antenna will be optimized. The fabrication and the measurement the proposed array antenna will be done.

## ACKNOWLEDGMENT

This research is funded by University of Transport and Communications (UTC) under grant number T2021-DT-005TĐ.

## REFERENCES

[1]. H. D. Nguyen, Research on application of intelligent transportation system (ITS) in operation management, traffic management and toll collection on Vietnam's expressway system, Project report, Institute of Transport science and technology, Hanoi, Vietnam, 2014 (in Vietnamese).

[2]. European Committee for Standardization, Road transport and traffic telematics - dedicated short- EN 12253:2004 - Road transport and traffic telematics - Dedicated short-range communication - (iteh.ai), (accessed 5 September 2022).

[3]. European Telecommunications Standards Institute, Harmonized European Standard (Telecommunications series) Intelligent Transport Systems (ITS), Radiocommunications equipment operating in the 5 855 MHz to 5 925 MHz frequency band, Harmonized EN covering the essential requirements of article 3.2 of the R&TTE Directive. SIST EN 302 571 V1.1.1:2008 - Intelligent Transport Systems (ITS) - Radiocommunications equipment (iteh.ai), (accessed 5 September 2022).

[4]. W. Liu, H. Ning, B. Wang, RFID Antenna Design of Highway ETC in ITS, in International Symposium on Antennas and Propagation & EM Theory, 2006. https://doi.org/ 10.1109/ISAPE.2006.353442

[5]. J. S. Jang, N. Hak, Y. W. Koo, J. K. Ha., Planar Array Antenna Design with Beam Shaping for ETCS-RSE, in Asia-Pacific Microwave Conference Proceedings, (2013) 694-696. https://doi.org/ 10.1109/APMC.2013.6695064

[6]. N. Rimbault, A. Sharaiha, S. Collardey, Very Low Profile Helix Antenna Feeding Resonant Cavity for ETC system, in International Symposium on Antenna Technology and Applied Electromagnetics, 2014.

[7]. T. Varum, J. N. Matos, R. Abreu, P. Pinho, Non-uniform microstrip antenna array for RxDSRC communications, in IEEE Antennas and Propagation Society International Symposium, 2014. https://doi.org/ 10.1109/APS.2014.6904862

[8]. Y. Zhao, Circular Polarized Fabry-Perot Resonator Antenna for Dedicated Short Range Communication, in IEEE International Wireless Symposium, 2014. https://doi.org/ 10.1109/IEEE-

IWS.2014.6864233
[9]. T. Varum, J. N. Matos, P. Pinho, R. Abreu, Non-uniform broadband circularly polarized antenna array for vehicular communications, IEEE Transactions on Vehicular Technology, 65 (2015) 7219-7227. https://doi.org/10.1109/TVT.2015.2500520
[10]. B. R. Franciscatto, A.C. Souza, C. Defay, T. T. Trang, T. P. Vuong, Design and implementation of a new low-power consumption DSRC transponder, Master Thesis, University Grenoble Alpes, France, 2014.
[11]. L. Yuan, H. Y. Xuan, L. Z. Wei, C. S. Ting, X. X. Ming, G. Jing, Design of a compact wideband CP metasurface antenna, international journal of rf and microwave computer-aided engineering, 30 (2020) e22332. https://doi.org/10.1002/mmce.22332
[12]. Y. Cao, Y. Cai, W. Cao, B. Xi, Z. Qian, T. Wu, L. Zhu, Broadband and high-gain microstrip patch antenna loaded with parasitic mushroom-type structure, IEEE antennas and wireless propagation letters, 18 (2019) 1405-1409. https://doi.org/10.1109/LAWP.2019.2917909
[13]. P. Xu, Z. Yan, T. Zhang, X. Yang, Broadband circularly polarized slot antenna array using a compact sequential-phase feeding network, Progress in electromagnetics research C, 47 (2014) 173-179. http://dx.doi.org/10.2528/PIERC14011610